Desalination and Water Treatment
www.deswater.com

doi: 10.5004/dwt.2020.25264

191 (2020) 11–20
July

Influence of hydraulic pressure on pore wetting of direct contact membrane distillation (DCMD)

Bomin Kim, Yongjun Choi, Jaehyun Ju, Jihyeok Choi, Sangho Lee*

School of Civil and Environmental Engineering, Kookmin University, 77 Jeongneung-ro, Seongbuk-Gu, Seoul, 02707, Republic of Korea, Tel. +82-2-910-4529; Fax: +82-2-910-4939; email: sanghlee@kookmin.ac.kr (S. Lee)

Received 23 August 2019; Accepted 29 November 2019

ABSTRACT

This paper presents the experimental results on the effect of hydraulic pressure on the wetting of membrane distillation (MD) membranes. Using $CaSO_4$ as a model foulant, a series of MD experiments were carried out by adjusting the feed and distillate pressure between 0.1 and 0.7 bar. The flux, electric conductivity of the distillate, rejection, and recovery was measured in each experiment. The rate of the conductivity increase (dE_c/dt) and the liquid entry pressure (LEP) were also estimated as quantitative measures for wetting propensity. Results showed that there was no wetting due to scale formation without the application of the external hydraulic pressure. As the feed pressure exceeds the distillate pressure, the wetting was accelerated. The recovery was higher when the distillate pressure was higher than the feed pressure. The rejection maintained high when the feed pressure was equal or less than the distillate pressure. The wetting by net pressure lower than the LEP is attributed to the existence of relatively large pores in the MD membrane.

Keywords: Membrane distillation (MD); Hydraulic pressure; Wetting; Fouling; Scale formation

1. Introduction

As the world population is continuously increasing, there are rising concerns about the scarcity of freshwater [1–3]. This has led to the implementation of seawater desalination, which has broadened its application into many countries all over the world [4]. Unfortunately, conventional desalination technologies such as multistage flash (MSF), multi-effect distillation (MED), and seawater reverse osmosis (SWRO) have limitations by their high energy demand and potential adverse impact on the marine environment due to the discharge of concentrated brines [5,6]. Accordingly, it is necessary to develop novel desalination techniques, which can utilize renewable energy sources and reduce the brine discharge [7–9].

One of the alternatives to the conventional desalination technologies is membrane distillation (MD). MD is a thermal desalination process using hydrophobic and microporous membrane [10,11]. Since MD may be operated under a lower feed water temperature than that of MSF or MED, it opens the possibility of renewable energy utilization [12]. Moreover, MD can process a feed water with high osmotic pressure (>100 bar), which makes SWRO impossible to be operated [13]. Accordingly, more fresh water can be obtained from the seawater by MD, thereby reducing the volume of the concentrated brine [14]. These advantages have sparked researches on the development of MD technologies [15–24].

However, MD has crucial issues associated with membrane fouling due to scale formation and pore wetting by water. Similar to other membrane processes, membrane fouling is an inevitable problem in MD [25–27]. As a result of fouling, the flux decreases, the quality of the permeated water deteriorates, and the recovery decreases [25,26,28–30]. In MD, scale formation by sparingly soluble salts such as $CaCO_3$ and $CaSO_4$ is a major reason to cause fouling [31,32]. As the feed solution becomes concentrated to a critical level

* Corresponding author.

Presented at the 12th International Desalination Workshop (IDW2019), 28–30 August 2019, Jeju, Korea

1944-3994/1944-3986

of saturation, the scale grows on the membrane surface or bulk crystal precipitates to the membrane [27,33]. This leads to the blockage of the membrane pores and reduction in the effective membrane area [34]. Consequently, a dramatic flux decline occurs due to scale formation. Operating temperature and hydrodynamic conditions have been reported to affect MD fouling due to scale formation [35].

MD also suffers from the potential problem of the pore wetting by the feed solution. Although MD membranes are hydrophobic and repel water, the pores of the membranes may be filled with water after a long-term operation [11]. If the membranes are exposed to high pressure, which exceeds the liquid entry pressure (LEP), the pore wetting may happen [36]. The presence of amphiphilic substance and fouling due to scale formation can accelerate the pore wetting by changing the physical and chemical properties of the membrane surfaces [36]. Once the pore wetting occurs, it is difficult to recover to the initial state [36–38]. A few studies have been done to overcome or mitigate the problems by the wetting, including the development of novel MD membranes [39], analysis of the wetting mechanisms [11], and recovery of the wetted pores by applying dewetting techniques [40,41].

Nevertheless, little attention has been paid yet to the effect of hydraulic pressure on the wetting of MD membranes under fouling conditions. During the operation of MD systems, the hydraulic pressure is applied either to the feed stream or distillate stream [42]. Since the pressure is lower than the liquid entry pressure, it will not cause wetting for clean MD membranes. But it is possible for MD membranes to be wetted if they are fouled by scales. Although a handful of works have considered the influence of the hydraulic pressure on flux, recovery, and rejection [42–46], to the best of our knowledge, few have examined how it affects MD membrane wetting under fouling conditions.

Accordingly, this study aimed at the elucidation of the effect of the hydraulic pressure on the wetting for MD membranes exposed to the feed solution containing scale-forming ions. The hydraulic pressure was put on the feed side as well as the distillate side and the propensity of the wetting was compared under various conditions. The hydraulic pressure on the feed and permeated side were varied within the range of 0.7 bar. Initial flux, recovery, rejection, and membrane wetting were compared in various hydraulic pressure conditions. LEP was also measured to evaluate the hydrophobicity of the membrane. The key questions to be answered in this study are: (1) What is the effect of the hydraulic pressure on the feed side on the flux and wetting due to scale formation?; (2) What is the effect of the hydraulic pressure in the permeate side on the flux and wetting due to scale formation?; and (3) How is the mechanism of wetting due to scale formation under the application of the hydraulic pressure?

2. Experimental methods

2.1. MD membranes

The hydrophobic and microporous membrane was used for the experiments. Membranes were made of polyvinylidene (PVDF) (GVHP, Merck Millipore, U.S.A.). The average pore size, thickness, and porosity were 0.22 and 125 µm, and 75%, respectively. The pore size distribution was also measured using a capillary flow porometry (CFP-1500-AFL, Porous Materials Inc., USA).

2.2. Feed solution

The solute used in this study was $CaSO_4$, which was purchased from Samchun Pure Chemical Co. Ltd., Korea. The $CaSO_4$ concentration of the feed solution was set to 2,000 mg/L. In each experiment, 1 L of the feed solution was used.

2.3. Hydraulic pressure conditions

In this study, the LEP of the membranes were directly measured using a device fabricated in the laboratory. The system consists of a high-pressure nitrogen cylinder, a pressure regulator, a pressure vessel, a pressure gauge, and a membrane holder. The applied pressure increased stepwise before the penetration of water through the membrane was observed. The measurements were triplicated to obtain reliable results. Details on this device are shown in our previous paper [41].

The LEP of the membrane used in this study was determined to be 1.8 ± 0.2 bar. If hydraulic pressure above the LEP is applied, water passes through the membrane pore. Therefore, the maximum hydraulic pressure was set to 0.7 bar, which is less than 40% of the LEP for the intact membrane. The experiments were carried out by varying the pressure on the feed side and the permeated side, respectively, as shown in Table 1. These operating conditions were selected based on our previous works [40–42].

2.4. Direct contact membrane distillation experiments

Fig. 1 illustrates a schematic diagram of the laboratory-scale setup for DCMD experiments. Pressure gauges were installed at the inlet and outlet of the membrane module, respectively. Hydraulic pressure was adjusted by installing valves at the outlets of the feed and permeate side. The membrane cell was made of acrylic resin and its

Table 1
Experimental sets to analyze the effect of feed and distillate pressures on MD wetting

Set No.	Pressure on feed side (bar)	Pressure on distillate side (bar)
1	0.1	0.1
2	0.1	0.4
3	0.1	0.7
4	0.4	0.1
5	0.4	0.4
6	0.4	0.7
7	0.7	0.1
8	0.7	0.4
9	0.7	0.7

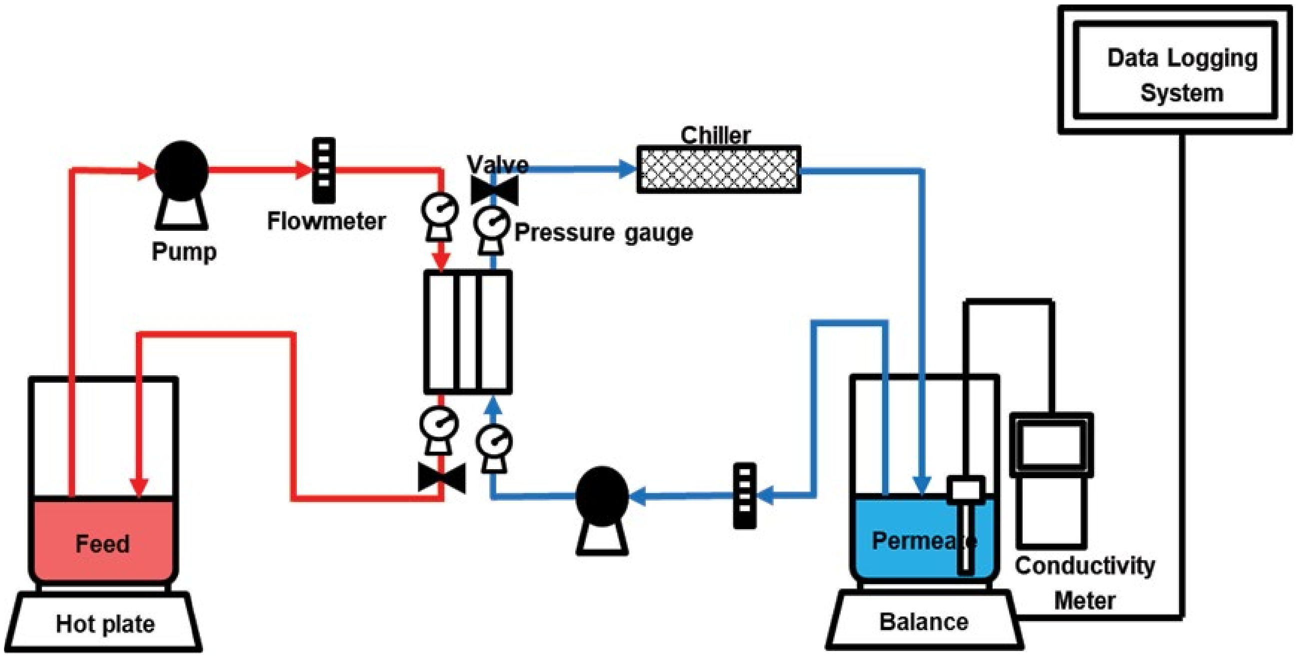

Fig. 1. Schematic diagram of the DCMD experiment.

depth, width, and length were 2, 20, and 60 mm, respectively. The effective membrane area was 0.0012 m^2. The temperature and flow rates were maintained at 60°C and 0.7 L/min for the feed and 20°C and 0.4 L/min for the distillate. The volumes of the feed solution and distillate were 1.0 and 1.5 L, respectively. Each experiment was conducted for 80 h. It was assumed that wetting occurs when the distillate conductivity exceeds 50 µS/cm. Since the permeate quality of 50 µS/cm corresponds to the rejection of about 98%, it was used as a practical criterion for membrane wetting.

2.5. Liquid entry pressure

LEP with the application in the MD process can be calculated as a first parameter to indicate how wettable a membrane is toward liquid solutions. Fig. 2 illustrates LEP equipment and the LEP equipment was manufactured by hand. A piston is located in the filtration cell, filling the water between the piston and the membrane. N_2 gas was used to increase the pressure in the piston. Therefore, the pressure is applied to the membrane. When water penetrates the membrane surface, the pressure is LEP.

3. Results and discussion

3.1. Effect of distillate pressure on wetting

The feed solution containing 2,000 mg/L $CaSO_4$ was treated by the MD membrane in the experimental setup in Fig. 1. The flux was measured to estimate the fouling propensity and the electric conductivity was monitored to examine the wetting property. First, the experiment was performed without applying hydraulic pressure to neither feed side nor distillate side. The changes in the flux and conductivity are presented as a function of the operation time in Fig. 3a. Initially, the flux was approximately 20 kg/m^2 h and maintained for about 15 h. After this time, the flux abruptly decreased due to $CaSO_4$ scale formation. As the feed solution is concentrated, surface blockage occurs from the point where $CaSO_4$ crystals occur, and the flux decreases drastically [27]. Nevertheless, the conductivity did not change significantly, suggesting that the wetting of the MD membrane did not occur. It is likely that the MD fouling did not cause the wetting under the condition in Fig. 3a.

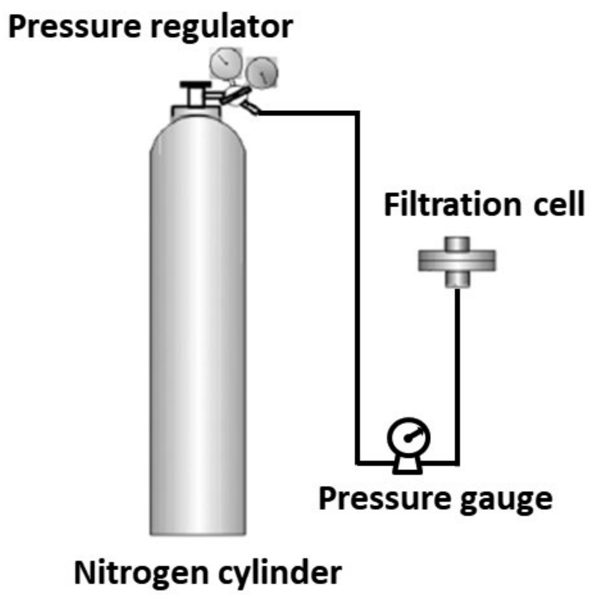

Fig. 2. Schematic diagram of liquid entry pressure (LEP) equipment.

(a)

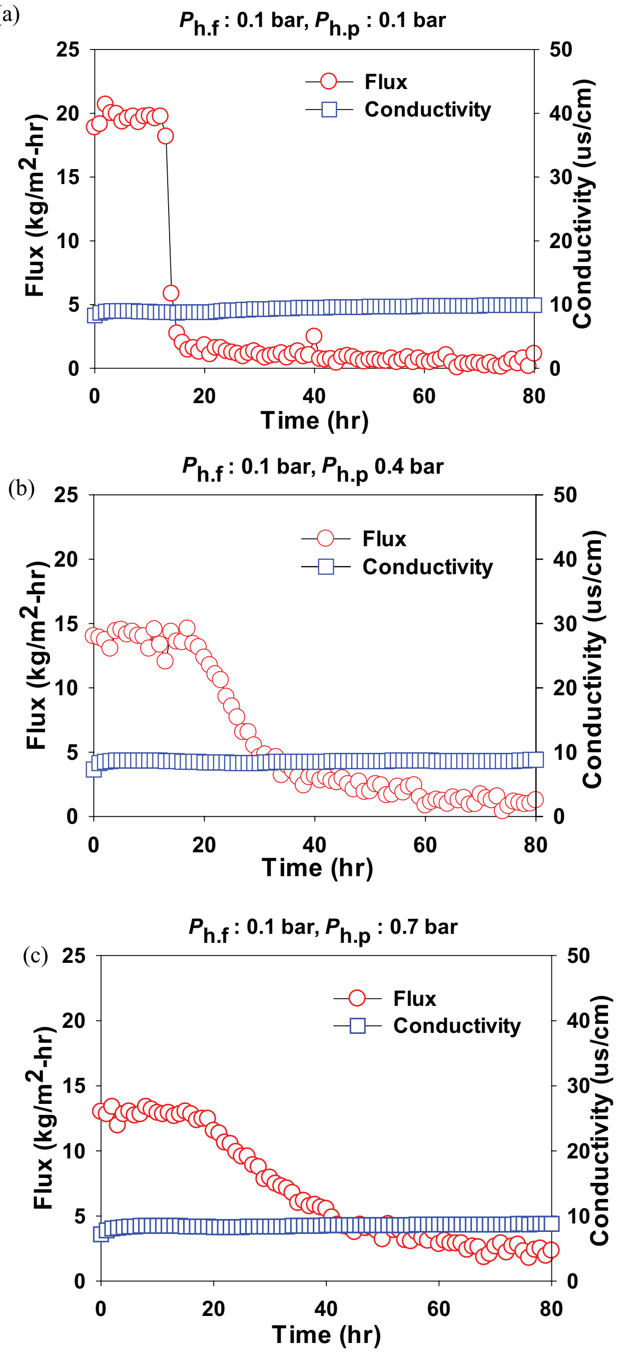

Fig. 3. Dependence of flux and electric conductivity of the distillate solution on time (a) $P_{h,f}$ = 0.1 bar and $P_{h,p}$ = 0.1 bar, (b) $P_{h,f}$ = 0.1 bar and $P_{h,p}$ = 0.4 bar, and (c) $P_{h,f}$ = 0.1 bar and $P_{h,p}$ = 0.7 bar.

As a next step, the pressure on the distillate side ($P_{h,p}$) increased to 0.4 and 0.7 bar, respectively. The feed pressure ($P_{h,f}$) was fixed at 0.1 bar, which is the same as Fig. 3a. When the distillate pressure was 0.4 bar, the flux was also reduced after a certain period of time as shown in Fig. 3b. However, the initial flux became lower by increasing the distillate pressure. A further increase in the distillate pressure led to a lower initial flux as illustrated in Fig. 3c. This may be attributed to the deformation of the membrane as reported by previous works in the literature [43,44,47]. Since the initial flux was reduced, the flux decline was less severe at higher distillate pressure. In addition, the conductivity of the distillate did not significantly increase with an increase in the distillate pressure, suggesting that there was no wetting induced by the distillate pressure.

3.2. Effect of feed pressure on wetting

The pressure on the feed side was also adjusted to examine its effect on wetting. Fig. 4 shows the results of the MD experiment with the feed pressure of 0.4 bar. The distillate pressure was controlled to 0.1, 0.4, and 0.7 bar, respectively. When the feed and distillate pressures were 0.4 and 0.1 bar, respectively (Fig. 4a), the flux decline was observed after 18 h with an increase in the conductivity of the distillate solution. After 80 h, the conductivity increased up to 30 mS/cm, indicating the occurrence of moderate wetting. Compared with Fig. 3a, the initial flux was slightly lower, which may be attributed to the membrane deformation, and the conductivity of the distillate solution became higher. It is evident that the wetting was induced by the feed pressure. In fact, the pressure applied here was far less than the LEP of this membrane (~ 2.0 bar) but resulted in wetting.

The effect of the feed pressure on wetting was affected by the distillate pressure. In Fig. 4b, the feed, and distillate pressures were set to 0.4 bar and a slight increase in the permeate conductivity was observed. Nevertheless, this was not considered as an occurrence of the wetting since the wetting criterion was set to 50 mS/cm. A further increase in the distillate pressure to 0.7 bar also resulted in the prevention of the wetting (Fig. 4c). These results imply that the net pressure difference between the feed and distillate sides is an important factor affecting the wetting. Although the feed pressure increases, wetting may not occur without the net pressure difference across the membrane. The wetting seems to happen as long as the feed pressure is higher than the distillate pressure.

A set of the MD experiments were also carried out with the feed pressure of 0.7 bar. When the net pressure was 0.6 bar, the wetting rapidly occurred as illustrated in Fig. 5a. With the net pressure of 0.3 bar, the wetting propensity was slightly reduced as indicated in Fig. 5b. Again, no wetting was found with the net pressure of 0 bar in Fig. 5c. These results also confirm the importance of the net pressure difference between the feed and distillate side for the occurrence of the wetting.

The effect of the pressure on the initial flux is summarized in Table 2. As mentioned earlier, the initial flux decreased with the net pressure difference. Regardless of the feed pressure, the initial flux was not changed with no net pressure difference. If the feed pressure is not equal to the distillate pressure, the initial flux was affected. Again, this can be explained by the effect of the membrane deformation [43,44,47].

3.3. Quantitative analysis of pressure effect

To further investigate the effect of the feed and distillate pressures on wetting, the rates of the conductivity increase (dE_c/dt) were calculated to estimate the wetting propensity. Linear regression was conducted to determine the slope of the curve for the distillate conductivity, which corresponds to dE_c/dt. As shown in Fig. 6, the slope of the curves was affected by the feed and distillate pressures. The slope becomes greater if the feed pressure is higher than that of the distillate. On the other hand, the slope is near zero if the distillate pressure is higher than that of the feed.

Table 3 summarizes dE_c/dt for different feed and distillate pressures. It should be noted that dE_c/dt decreases with the distillate pressure. For instance, dE_c/dt is 0.0169 mS/cm at the feed pressure of 0.1 bar and the distillate pressure of 0.1 bar. An increase in the distillate pressure to 0.4 and 0.7 bar results in a reduced value for dE_c/dt, which is 0.003 mS/cm. Similar results were obtained for the other feed pressures. On the other hand, dE_c/dt

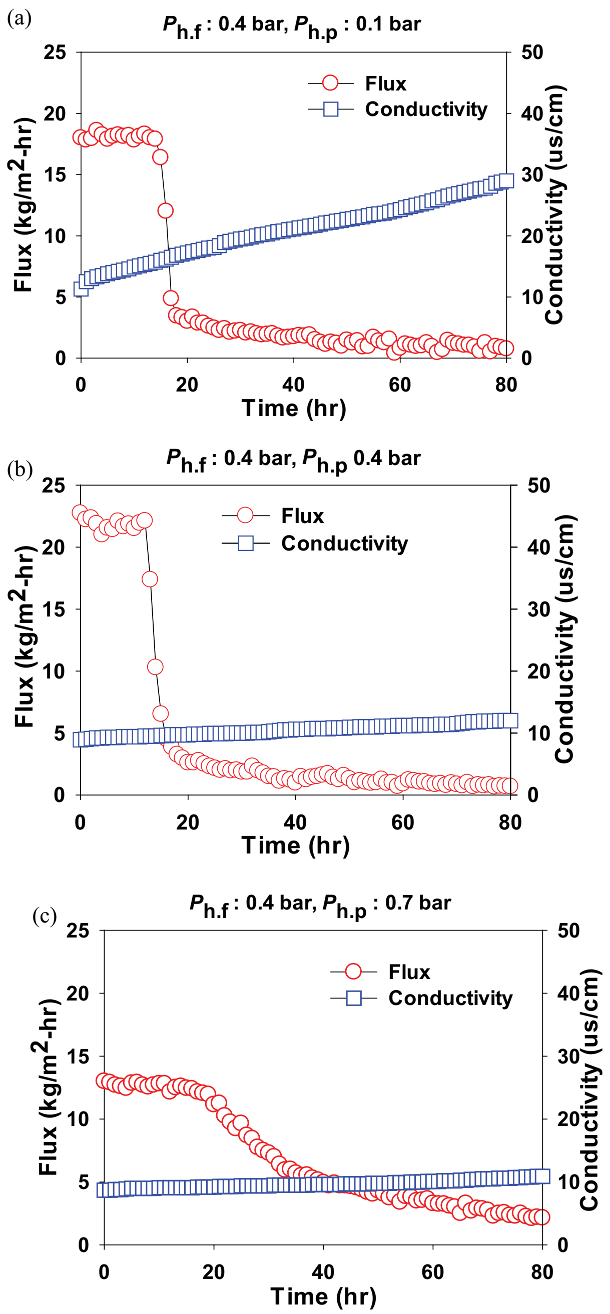

Fig. 4. Dependence of flux and electric conductivity of the distillate solution on time (a) $P_{h,f}$ = 0.4 bar and $P_{h,p}$ = 0.1 bar, (b) $P_{h,f}$ = 0.4 bar and $P_{h,p}$ = 0.4 bar, and (c) $P_{h,f}$ = 0.4 bar and $P_{h,p}$ = 0.7 bar.

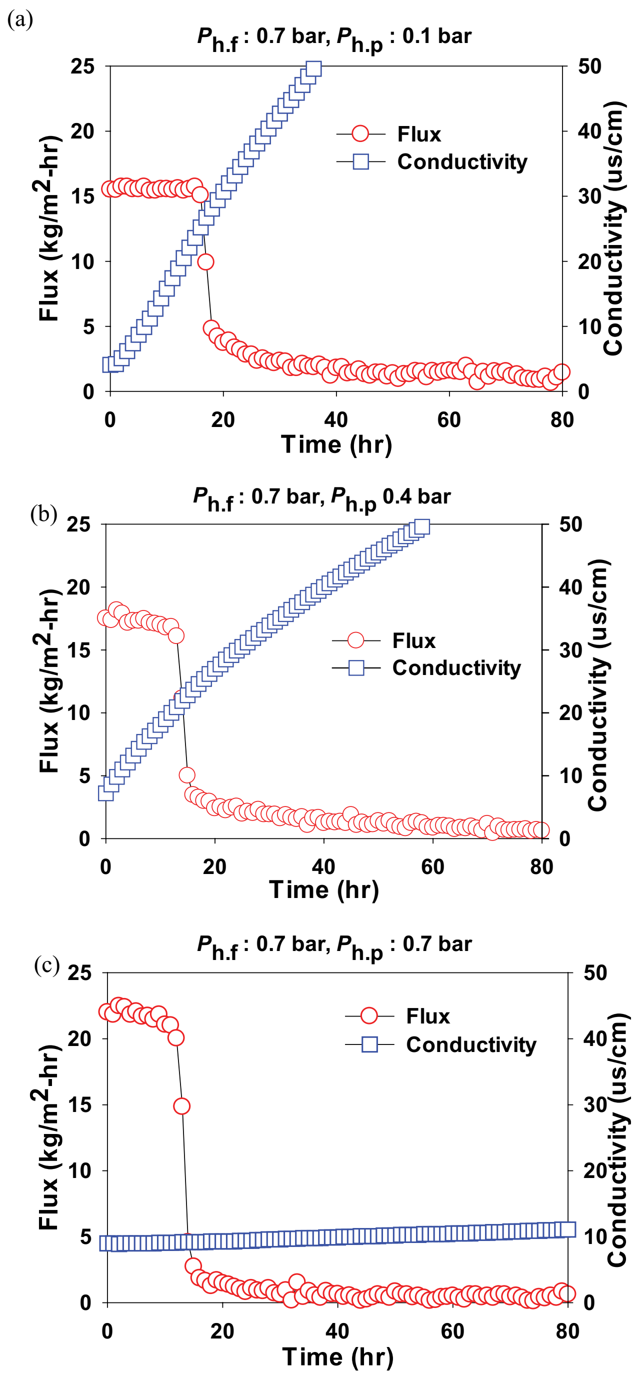

Fig. 5. Dependence of flux and electric conductivity of the distillate solution on time (a) $P_{h,f}$ = 0.7 bar and $P_{h,p}$ = 0.1 bar, (b) $P_{h,f}$ = 0.7 bar and $P_{h,p}$ = 0.4 bar, and (c) $P_{h,f}$ = 0.7 bar and $P_{h,p}$ = 0.7 bar.

increases with the feed pressure. For instance, as the feed pressure increases from 0.1 to 0.4 bar, dE_c/dt increases from 0.0169 to 0.196 mS/cm at the distillate pressure of 0.1 bar. There are similar trends for the other distillate pressures.

3.4. Effect of pressure on recovery

The volume concentration factor (VCF) is the amount that the feed stream has been reduced in volume from the initial volume. VCF should be calculated based only on the volume corresponding to the following equation.

$$\text{VCF} = \frac{\text{Total starting feed volume added to the operation}}{\text{current retentate volume}} \quad (1)$$

The changes in flux with VCF are illustrated in Fig. 7 under different feed and distillate pressures. The final VCF and recovery are listed in Table 4. When the feed and distillate pressures were the same, the initial flux was high, leading to a more rapid flux decline due to scale formation. Accordingly, the recovery of the distillate was reduced under these conditions. On the other hand, the recovery increased if the distillate pressure is higher than the feed pressure. A reduction in the initial flux, which leads to a retardation in the flux decline, is the major reason for these phenomena. The initial flux was reduced when the feed pressure is higher than the distillate pressure, which did not result in increased recovery. This is because the wetting also occurred under these conditions, which causes an additional flux decline.

Table 2
Comparison of initial flux under various pressure conditions

$P_{h,f}$ \ $P_{h,p}$	0.1 bar	0.4 bar	0.7 bar
0.1 bar	20 L/m² h	15 L/m² h	13 L/m² h
0.4 bar	18 L/m² h	22 L/m² h	13 L/m² h
0.7 bar	15 L/m² h	17 L/m² h	22.5 L/m² h

3.5. Effect of pressure on rejection

After each MD experiment, the solute rejection was measured, which is related to the degree of wetting. As shown in Fig. 8, the rejection was higher when the feed pressure was

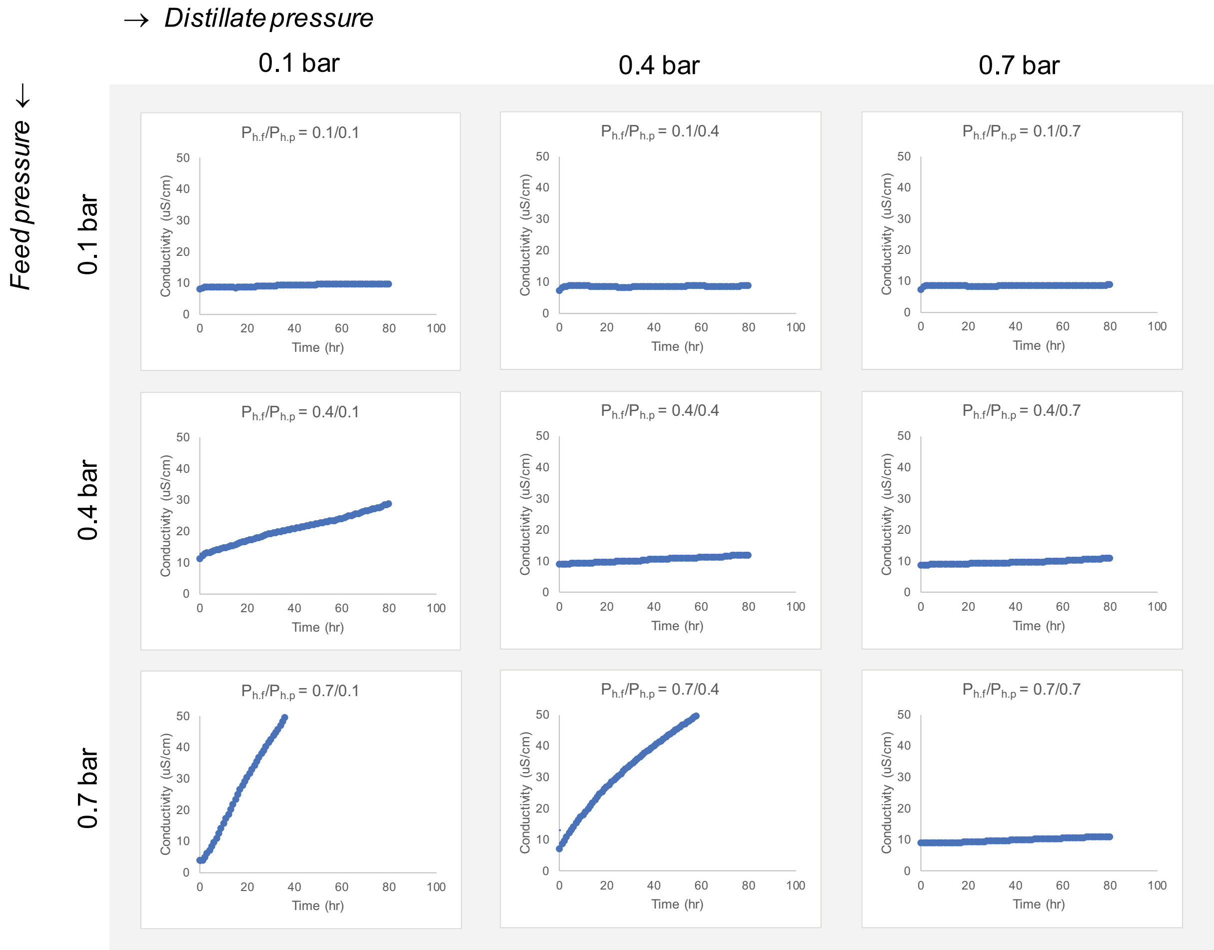

Fig. 6. Comparison of electric conductivity of distillate solution with different $P_{h,f}$ and $P_{h,p}$.

Table 3
Comparison of the rate of conductivity change (dEc/dt) under various pressure conditions

$P_{h,f}$ \ $P_{h,p}$	0.1 bar	0.4 bar	0.7 bar
0.1 bar	0.0169 mS/cm-h	0.003 mS/cm-h	0.003 mS/cm-h
0.4 bar	0.196 mS/cm-h	0.0368 mS/cm-h	0.0242 mS/cm-h
0.7 bar	1.33 mS/cm-h	0.623 mS/cm-h	0.028 mS/cm-h

Table 4
Summarized the VCF and recovery at various hydraulic pressure conditions

$P_{h,f}$ \ $P_{h,p}$		0.1 bar	0.4 bar	0.7 bar
0.1 bar	VCF	1.65	2.47	2.77
	Recovery	39.26%	59.57%	63.86%
0.4 bar	VCF	1.70	1.86	2.80
	Recovery	41.20%	43.17%	64.36%
0.7 bar	VCF	1.58	1.62	1.60
	Recovery	37.41%	38.50%	37.42%

Table 5
Summarized the VCF and recovery at various hydraulic pressure conditions

$P_{h.f}$ \ $P_{h.p}$	0.1 bar	0.4 bar	0.7 bar
0.1 bar	99.92 %	99.93 %	99.92 %
0.4 bar	99.16 %	99.85 %	99.90 %
0.7 bar	95.00 %	97.49 %	99.90 %

Table 6
Summarized the LEP at various hydraulic pressure conditions

$P_{h,f}$ \ $P_{h,p}$	0.1 bar	0.4 bar	0.7 bar
0.1 bar	1.70 bar	1.51 bar	1.57 bar
0.4 bar	1.02 bar	1.53 bar	1.64 bar
0.7 bar	0.51 bar	1.15 bar	1.57 bar

equal or less than the distillate pressure (set 1, set 2, set 3, set 5, set 6, and set 9). A decrease in the rejection was found in the case that the feed pressure was higher than the distillate pressure (set 4, set 6, and set 7). These trends are clearly demonstrated in Table 5. The rejection is lower at higher feed pressure. The results also qualitatively match with those in Table 3.

3.6. LEP under various hydraulic conditions

In general, the contact angle is an important property related to MD membrane wetting. However, if scaling occurs

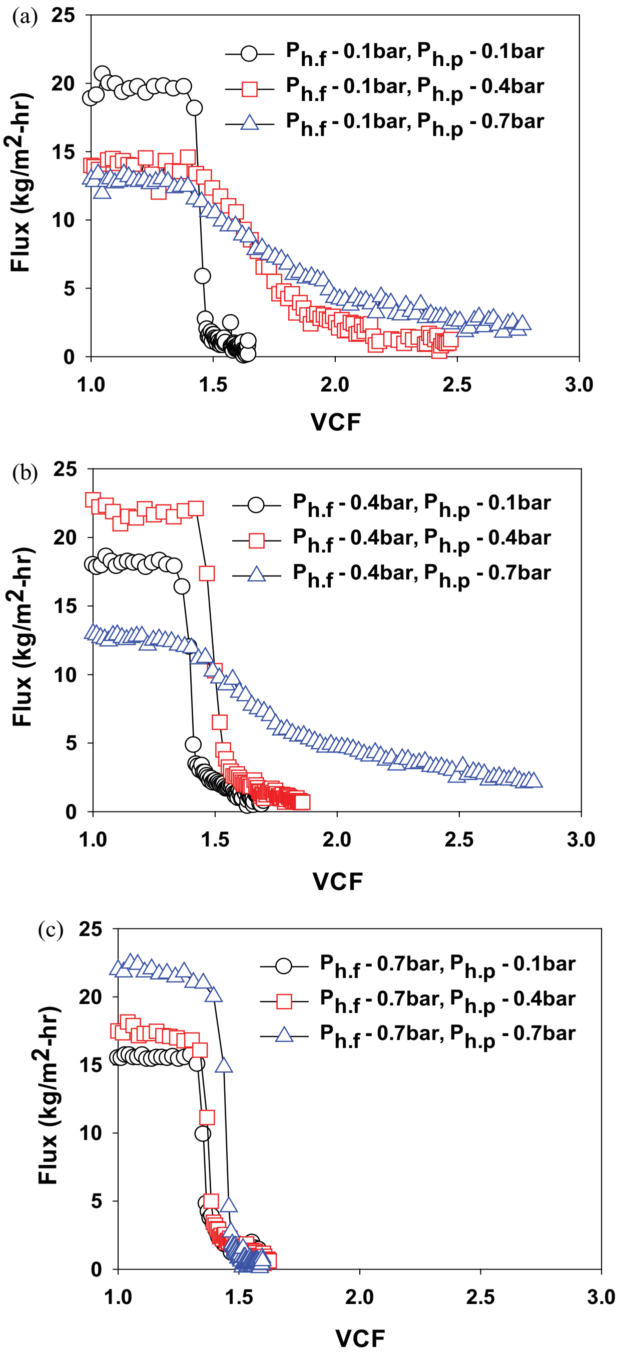

Fig. 7. Comparison of flux decline with VCF under various pressure conditions. (a) $P_{h,f}$ = 0.1, (b) $P_{h,f}$ = 0.4 bar, and (c) $P_{h,f}$ = 0.7 bar.

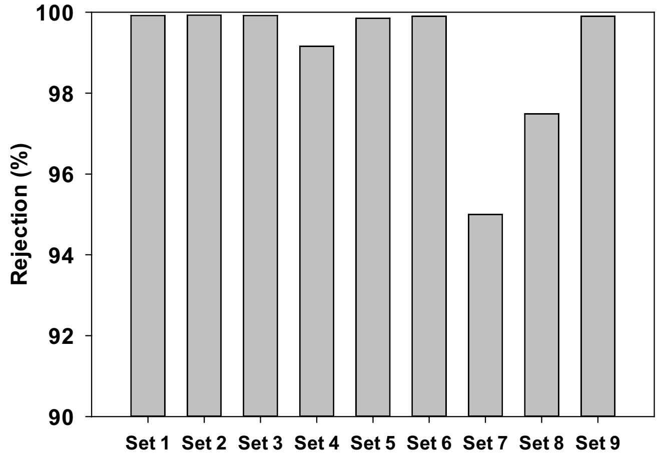

Fig. 8. Comparison of rejection. (Set 1) $P_{h,f}$ = 0.1 bar and $P_{h,p}$ = 0.1 bar, (set 2) $P_{h,f}$ = 0.1 bar and $P_{h,p}$ = 0.4 bar, (set 3) $P_{h,f}$ = 0.1 bar and $P_{h,p}$ = 0.7 bar, (set 4) $P_{h,f}$ = 0.4 bar and $P_{h,p}$ = 0.1 bar, (set 5) $P_{h,f}$ = 0.4 bar and $P_{h,p}$ = 0.4 bar, (set 6) $P_{h,f}$ = 0.4 bar and $P_{h,p}$ = 0.7 bar, (set 7) $P_{h,f}$ = 0.7 bar and $P_{h,p}$ = 0.1 bar, (set 8) $P_{h,f}$ = 0.7 bar and $P_{h,p}$ = 0.4 bar, and (set 9) $P_{h,f}$ = 0.7 bar and $P_{h,p}$ = 0.7 bar.

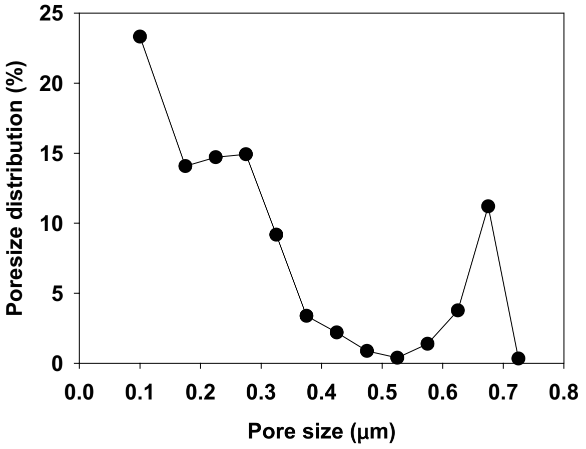

Fig. 9. Pore size distribution of virgin membrane.

on the membrane surface, the measurement of the contact angle is not meaningful. This is because inorganic scales are generally hydrophilic, leading to a reduced contact angle regardless of the membrane wetting. In our experiments, the contact angles ranged from 0° to 20° and there were no correlations between the contact angle and the membrane wetting.

Accordingly, the LEP was measured to examine the membrane wetting instead of the contact angle. Table 6 summarizes the LEP of the membranes after the experiments. The LEP of the virgin membrane was measured to be 1.8 bar. After the experiments, the LEP was reduced, ranging from 0.51 to 1.70 bar. The highest LEP was obtained when the feed and permeate pressures were 0.1 bar, indicating that the wetting is less severe under lower pressures. The lowest LEP was found at the feed and permeate pressures were 0.7 and 0.1 bar, respectively. It is evident that the high-pressure difference between the feed and the permeate accelerated the wetting. When the pressure difference was 0.3 bar, the LEP was also relatively low, which can be also attributed to the effect of the pressure difference. In other cases, the LEP was only slightly reduced. These results indicate that the LEP of the membrane is affected by the hydraulic pressure difference in the MD experiments.

3.7. Pore size distribution and wetting by pressure

It is interesting to note that wetting occurred with the application of the pressure less than the LEP. As listed in Table 5, the rejection ranges from 95.00% to 99.16% with the occurrence of wetting. This implies that the wetting induced by the pressure less than the LEP was moderate, indicating that only a small portion of the pores was wetted. Since the pores in the MD membrane are not uniform, the larger pores seem to be preferentially wetted. To confirm this hypothesis, the pore size distribution of the intact membrane was measured as illustrated in Fig. 9. The nominal pore size of this membrane is 0.22 μm and the average pore size determined by the analysis is 0.243 μm, which shows a reasonable match. However, there are also larger pores ranging from 0.6 to 0.7 μm in Fig. 9, which are more vulnerable to wetting. It is likely that these large pores are wetted with the application of the pressure together with scale-forming ions. Since the portion of these pores is not high, only partial wetting occurred under the conditions in this study.

4. Conclusions

This study examined the effect of the hydraulic pressure on the wetting for MD membranes and the conclusions are summarized as follows:

- Without the external pressure, the MD membrane did not experience wetting by the fouling due to $CaSO_4$ scale formation. The application of hydraulic pressure on the distillate side did not result in the wetting of the MD membrane. The wetting occurred only when both the feed pressure and the net pressure difference between the feed and the distillate solutions were high.
- The initial flux decreased with the net pressure difference between the feed and the distillate solutions. Regardless of the feed pressure, the initial flux was not changed with no net pressure difference.
- The rejection and recovery maintained high when the feed pressure was equal or less than the distillate pressure. They were reduced if the feed pressure was higher than the distillate pressure.

Acknowledgment

This work was supported by the Korea Institute of Energy Technology Evaluation and Planning (KETEP) and the Ministry of Trade, Industry & Energy (MOTIE) of the Republic of Korea (No. 20183010141130).

References

[1] W. Li, X. Hai, L. Han, J. Mao, M. Tian, Does urbanization intensify regional water scarcity?, evidence and implications from a megaregion of China, J. Cleaner Prod., (2019) 118592.

[2] Z. Xu, X. Chen, S.R. Wu, M. Gong, Y. Du, J. Wang, Y. Li, J. Liu, Spatial-temporal assessment of water footprint, water scarcity, and crop water productivity in a major crop production region, J. Cleaner Prod., 224 (2019) 375–383.
[3] A.V. Veettil, A.K. Mishra, Potential influence of climate and anthropogenic variables on water security using blue and green water scarcity, Falkenmark index, and freshwater provision indicator, J. Environ. Manage., 228 (2018) 346–362.
[4] I. Bremere, M. Kennedy, A. Stikker, J. Schippers, How water scarcity will effect the growth in the desalination market in the coming 25 years, Desalination, 138 (2001) 7–15.
[5] T.N. Bitaw, K. Park, J. Kim, J.W. Chang, D.R. Yang, Low-recovery, -energy-consumption, -emission hybrid systems of seawater desalination: energy optimization and cost analysis, Desalination, 468 (2019) 114085.
[6] H. Frank, K.E. Fussmann, E. Rahav, E. Bar Zeev, Chronic effects of brine discharge form large-scale seawater reverse osmosis desalination facilities on benthic bacteria, Water Res., 151 (2019) 478–487.
[7] A. Mollahosseini, A. Abdelrasoul, S. Sheibany, M. Amini, S.K. Salestan, Renewable energy-driven desalination opportunities – a case study, J. Environ. Manage., 239 (2019) 187–197.
[8] A. Alkaisi, R. Mossad, A. Sharifian-Barforoush, A review of the water desalination systems integrated with renewable energy, Energy Procedia, 110 (2017) 268–274.
[9] A. Panagopoulos, K.-J. Haralambous, M. Loizidou, Desalination brine disposal methods and treatment technologies – a review, Sci. Total Environ., 693 (2019) 133545.
[10] M. Khayet, Membranes and theoretical modeling of membrane distillation: a review, Adv. Colloid Interface Sci., 164 (2011) 56–88.
[11] M. Rezaei, D.M. Warsinger, M.C. Duke, T. Matsuura, W.M. Samhaber, Wetting phenomena in membrane distillation: mechanisms, reversal, and prevention, Water Res., 139 (2018) 329–352.
[12] G. G, A. G, I. Af, Perspective of renewable desalination by using membrane distillation, Chem. Eng. Res. Des., 144 (2019) 520–537.
[13] S. Lee, J. Choi, Y.-G. Park, H. Shon, C.H. Ahn, S.-H. Kim, Hybrid desalination processes for beneficial use of reverse osmosis brine: current status and future prospects, Desalination, 454 (2019) 104–111.
[14] R.A. Tufa, E. Curcio, E. Brauns, W. van Baak, E. Fontananova, G. Di Profio, Membrane distillation and reverse electrodialysis for near-zero liquid discharge and low energy seawater desalination, J. Membr. Sci., 496 (2015) 325–333.
[15] B. Ashoor, S. Mansour, A. Giwa, V. Dufour, S. Hasan, Principles and applications of direct contact membrane distillation (DCMD): a comprehensive review, Desalination, 398 (2016) 222–246.
[16] F. Eleiwi, N. Ghaffour, A.S. Alsaadi, L. Francis, T.M. Laleg-Kirati, Dynamic modeling and experimental validation for direct contact membrane distillation (DCMD) process, Desalination, 384 (2016) 1–11.
[17] Y. Yang, D. Rana, T. Matsuura, C.Q. Lan, The heat and mass transfer of vacuum membrane distillation: effect of active layer morphology with and without support material, Sep. Purif. Technol., 164 (2016) 56–62.
[18] F.A. Banat, F.A.A. Al-Rub, R. Jumah, M. Al-Shannag, Modeling of desalination using tubular direct contact membrane distillation modules, Sep. Sci. Technol., 34 (1999) 2191–2206.
[19] L. Francis, N. Ghaffour, A.S. Alsaadi, S.P. Nunes, G.L. Amy, Performance evaluation of the DCMD desalination process under bench scale and large scale module operating conditions, J. Membr. Sci., 455 (2014) 103–112.
[20] Q.L. Ve, K. Rahaoui, M. Bawahab, H. Faqeha, A. Date, A. Faghih, A. Akbarzadeh, An experimental heat transfer investigation of using spacer in direct contact membrane distillation, Energy Procedia, 160 (2019) 223–230.
[21] R. Schofield, A. Fane, C. Fell, Heat and mass transfer in membrane distillation, J. Membr. Sci., 33 (1987) 299–313.
[22] J. Zhang, S. Gray, Modeling heat and mass transfers in DCMD using compressible membranes, J. Membr. Sci., 387 (2012) 7–16.
[23] C.-C. Wang, On the heat transfer correlation for membrane distillation, Energy Convers. Manage., 52 (2011) 1968–1973.
[24] M.M. Damtie, Y.C. Woo, B. Kim, K.-D. Park, R.H. Hailemariam, H.K. Shon, J.-S. Choi, Analysis of mass transfer behavior in membrane distillation: mathematical modeling under various conditions, Chemosphere, 236 (2019) 124289.
[25] M. Gryta, Fouling in direct contact membrane distillation process, J. Membr. Sci., 325 (2008) 383–394.
[26] O.R. Lokare, S. Tavakkoli, S. Wadekar, V. Khanna, R.D. Vidic, Fouling in direct contact membrane distillation of produced water from unconventional gas extraction, J. Membr. Sci., 524 (2017) 493–501.
[27] T. Zou, X. Dong, G. Kang, M. Zhou, M. Li, Y. Cao, Fouling behavior, and scaling mitigation strategy of $CaSO_4$ in submerged vacuum membrane distillation, Desalination, 425 (2018) 86–93.
[28] L.D. Nghiem, T. Cath, A scaling mitigation approach during direct contact membrane distillation, Sep. Purif. Technol., 80 (2011) 315–322.
[29] M. Aslam, A. Charfi, G. Lesage, M. Heran, J. Kim, Membrane bioreactors for wastewater treatment: a review of mechanical cleaning by scouring agents to control membrane fouling, Chem. Eng. J., 307 (2017) 897–913.
[30] F.E. Ahmed, B.S. Lalia, R. Hashaikeh, Membrane-based detection of wetting phenomenon in direct contact membrane distillation, J. Membr. Sci., 535 (2017) 89–93.
[31] F. Kiefer, A. Präbst, T. Sattelmayer, Membrane scaling in vacuum membrane distillation-Part 2: crystallization kinetics and process performance, J. Membr. Sci., 590 (2019) 117293.
[32] Z. Xiao, Z. Li, H. Guo, Y. Liu, Y. Wang, H. Yin, X. Li, J. Song, L.D. Nghiem, T. He, Scaling mitigation in membrane distillation: from superhydrophobic to slippery, Desalination, 466 (2019) 36–43.
[33] Y. Choi, G. Naidu, S. Lee, S. Vigneswaran, Recovery of sodium sulfate from seawater brine using fractional submerged membrane distillation crystallizer, Chemosphere, 238 (2020) 124641.
[34] F. He, J. Gilron, H. Lee, L. Song, K.K. Sirkar, Potential for scaling by sparingly soluble salts in crossflow DCMD, J. Membr. Sci., 311 (2008) 68–80.
[35] D.M. Warsinger, E.W. Tow, J. Swaminathan, Theoretical framework for predicting inorganic fouling in membrane distillation and experimental validation with calcium sulphate, J. Membr. Sci., 528 (2017) 381–390.
[36] M.R. Choudhury, N. Anwar, D. Jassby, M.S. Rahaman, Fouling and wetting in the membrane distillation driven wastewater reclamation process–a review, Adv. Colloid Interface Sci., 269 (2019) 370–399.
[37] D. Hou, C. Ding, C. Fu, D. Wang, C. Zhao, J. Wang, Electrospun nanofibrous omniphobic membrane for anti-surfactant-wetting membrane distillation desalination, Desalination, 468 (2019) 114068.
[38] W.-U. Rehman, A. Muhammad, M. Younas, C. Wu, Y. Hu, J. Li, Effect of membrane wetting on the performance of PVDF and PTFE membranes in the concentration of pomegranate juice through osmotic distillation, J. Membr. Sci., 584 (2019) 66–78.
[39] Z. Wang, S. Lin, Membrane fouling and wetting in membrane distillation and their mitigation by novel membranes with special wettability, Water Res., 112 (2017) 38–47.
[40] Y. Shin, J. Choi, T. Lee, J. Sohn, S. Lee, Optimization of dewetting conditions for hollow fiber membranes in vacuum membrane distillation, Desal. Water Treat., 57 (2016) 7582–7592.
[41] Y. Shin, H. Cho, J. Choi, Y. Sun Jang, Y.-J. Choi, J. Sohn, S. Lee, J. Choi, Application of response surface methodology (RSM) in the optimization of dewetting conditions for flat sheet membrane distillation (MD) membranes, Desal. Water Treat., 57 (2016) 10020–10030.
[42] S.-M. Park, S. Lee, Influence of hydraulic pressure on performance deterioration of direct contact membrane distillation (DCMD) process, Membranes, 9 (2019) 37.

[43] P. Yazgan-Birgi, M.I.H. Ali, H.A. Arafat, Comparative performance assessment of flat sheet and hollow fiber DCMD processes using CFD modelling, Sep. Purif. Technol., 212 (2019) 709–722.
[44] J. Zhang, S. Gray, Effect of applied pressure on performance of PTFE membrane in DCMD, J. Membr. Sci., 369 (2011) 514–525.
[45] Z. Yuan, L. Wei, J.D. Afroze, K. Goh, Y. Chen, Y. Yu, Q. She, Y. Chen, Pressure-retarded membrane distillation for low-grade heat recovery: the critical roles of pressure-induced membrane deformation, J. Membr. Sci., 579 (2019) 90–101.
[46] I. Hitsov, L. Eykens, W. De Schepper, K. De Sitter, C. Dotremont, I. Nopens, Full-scale direct contact membrane distillation (DCMD) model including membrane compaction effects, J. Membr. Sci., 524 (2017) 245–256.
[47] X. Chen, C. Boo, N.Y. Yip, Low-temperature heat utilization with vapor pressure-driven osmosis: impact of membrane properties on mass and heat transfer, J. Membr. Sci., 588 (2019) 117181.